

PROCEEDINGS OF SPIE

[SPIDigitalLibrary.org/conference-proceedings-of-spie](https://spiedigitallibrary.org/conference-proceedings-of-spie)

Detectors based on Pd-doped and PdO-functionalized ZnO nanostructures

V. Postica, O. Lupan, N. Ababii, M. Hoppe, R. Adelung, et al.

V. Postica, O. Lupan, N. Ababii, M. Hoppe, R. Adelung, L. Chow, V. Sontea, P. Aschehoug, V. Viana, Th. Pauporte, "Detectors based on Pd-doped and PdO-functionalized ZnO nanostructures," Proc. SPIE 10533, Oxide-based Materials and Devices IX, 105332T (23 February 2018); doi: 10.1117/12.2294945

SPIE.

Event: SPIE OPTO, 2018, San Francisco, California, United States

Detectors based on Pd-doped and PdO-functionalized ZnO nanostructures

V. Postica,¹ O. Lupan,^{1,2,3} N. Ababii,¹ M. Hoppe,³ R. Adelung,³
L. Chow,⁴ V. Sontea,¹ P. Aschehoug,² B. Viana,² Th. Pauporté²

¹ Department of Microelectronics and Biomedical Engineering, Technical University of Moldova, 168 Stefan cel Mare Blvd., MD-2004, Chisinau, Republic of Moldova

² PSL Research University, Chimie ParisTech-CNRS, Institut de Recherche de Chimie Paris, UMR8247, 11 rue P. et M. Curie, 75005 Paris, France

³ Functional Nanomaterials, Institute for Materials Science, Kiel University, 24143 Kiel, Germany

⁴ Department of Physics, University of Central Florida, Orlando, FL 32816-2385, USA

ABSTRACT

In this work, zinc oxide (ZnO) nanostructured films were grown using a simple synthesis from chemical solutions (SCS) approach from aqueous baths at relatively low temperatures (< 95 °C). The samples were doped with Pd (0.17 at% Pd) and functionalized with PdO nanoparticles (NPs) using the PdCl₂ aqueous solution and subsequent thermal annealing at 650 °C for 30 min. The morphological, micro-Raman and optical properties of Pd modified samples were investigated in detail and were demonstrated to have high crystallinity. Gas sensing studies unveiled that compared to pure ZnO films, the Pd-doped ZnO (ZnO:Pd) nanostructured films showed a decrease in ethanol vapor response and slight increase in H₂ response with low selectivity. However, the PdO-functionalized samples showed excellent H₂ gas sensing properties with possibility to detect H₂ gas even at room temperature (gas response of ~ 2). Up to 200 °C operating temperature the samples are highly selective to H₂ gas, with highest response of ~ 12 at 150 °C. This study demonstrates that surface functionalization of *n*-ZnO nanostructured films with *p*-type oxides is very important for improvement of gas sensing properties.

Keywords: ZnO, nanostructured films, hydrogen gas, gas sensor.

1. INTRODUCTION

The common fossil fuels such as coal, natural gas, oil/petroleum are the main sources of energy nowadays. However, this type of energy is limited, non-renewable and has a big impact on air pollution. Therefore, in recent years a high demand for green and renewable energy sources is emerging. In this context, hydrogen gas is expected to become a new green and renewable energy source for different applications, such as aerospace, automobiles, households etc., in form of fuel cells¹. The main advantage of hydrogen gas is the abundance on Earth (less than 1% is presented as molecular H₂ gas)¹. However, due to problems with hydrogen-storage and because H₂ is an extremely dangerous gas, its use was limited and was not widely implemented in industry¹⁻². Therefore, detection of H₂ is very important in many fields.

As an *n*-type metal oxide, ZnO is an excellent material for use in chemiresistive detection of different reducing and oxidizing gases³. However, the ZnO has low selectivity to H₂ gas⁴ which is why different methods to improve the H₂ gas sensing properties of ZnO micro- and nanostructures were proposed⁵. Among them, the doping and surface functionalization with noble metals, especially Pd and PdO, were demonstrated to be highly efficient for the improvement of H₂ gas selectivity and for the reduction of the operating temperature down to room temperature^{2,5-6}. For example, Lupan *et al.* integrated a single Pd modified ZnO nanowire for the fabrication of a highly selective and sensitive H₂ gas nanosensor⁷. However, in the case of ZnO nanostructured films the high performances are harder to achieve due to low surface-to-volume ratio of films compared to different nanostructures such as nanowires, nanobelts, etc.⁸. ZnO nanostructured films can be grown by different methods such as spray pyrolysis, chemical bath deposition,

electrochemical deposition, etc.⁹⁻¹⁰. Nevertheless, the films have many advantages such as the possibility of controlled doping with different metals, high dependence on surface adsorbed species, and excellent adhesion to the substrate¹¹.

In this work, the ZnO nanostructured films were doped with Pd and then functionalized with PdO nanoparticles using a PdCl₂ aqueous solution. The morphological, micro-Raman and optical properties were investigated in detail. Compared to pristine ZnO and ZnO:Pd samples, the PdO-modified nanostructured films showed improved H₂ gas sensing properties that can detect H₂ gas even at room temperature. This is hard to achieve in the case of nanostructured films, but the PdO-modified films have an incomplete recovery to the initial electrical baseline. This study demonstrates the importance of surface functionalization of metal oxides for high performance gas sensing applications.

2. MATERIAL SYNTHESIS AND DEVICE STRUCTURES FABRICATION.

The Pd-doped ZnO nanostructured films were synthesized via a simple synthesis from chemical solutions (SCS) approach from aqueous bath as was previously reported¹¹⁻¹². The Pd-doping was achieved by adding 45 mM of PdCl₂ (Alfa Aesar) in the complex solution. All chemicals were of analytical grade without further purification. The post-growth annealing such as conventional thermal annealing (TA) in electrical furnace or rapid thermal annealing (RTA) was performed to increase the crystallinity of the samples¹³. The morphological, structural and optical characterization of the samples was performed as was reported previously^{7, 11-12}. The EDX analysis showed a 0.17 at.% Pd content in ZnO:Pd nanostructured films. The thickness of the films in this study is ~ 1.2 μm, which was measured by SEM in cross section (not shown).

The surface functionalization with PdO was achieved as followed: ZnO:Pd nanostructured films were vertically immersed into the 45 mM of PdCl₂ aqueous solution for 5 min, followed by TA at 650 °C for 30 min.

The sensor structure was fabricated using the same method reported in previous works^{11, 14}. The gold contacts with 170 nm thickness were sputtered on already deposited nanostructured films through a metal mask with meander configuration forming the Au/ZnO:Pd/Au structure. The gas sensing measurement procedure was performed as was reported previously¹⁴⁻¹⁶.

3. RESULTS AND DISCUSSIONS

Figure 1(a) shows a typical SEM image of as-grown ZnO:Pd nanostructured film at low magnification. As can be observed, the film is composed of columnar type grains which completely cover the glass substrate. No agglomerations were observed even at extensive-surface observations (not shown).

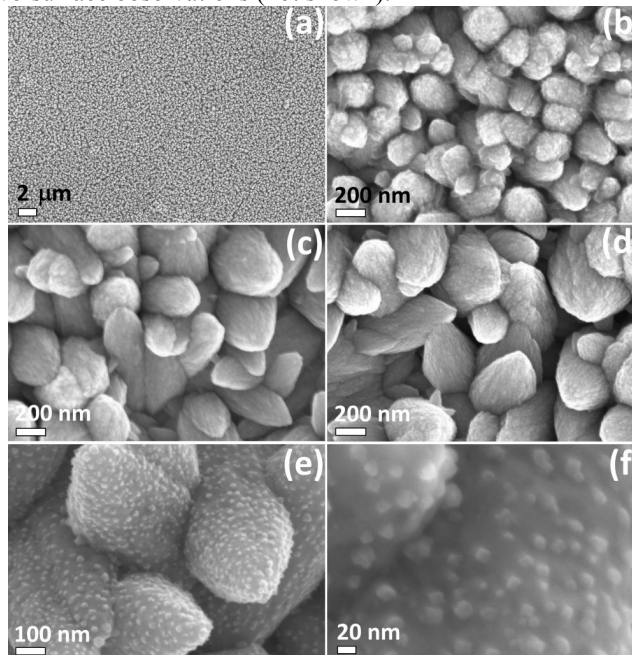


Figure 1. (a) Low magnification SEM image of an as-grown ZnO:Pd nanostructured film. SEM images at higher magnification of ZnO:Pd nanostructured film: (b) as-grown; (c) treated with TA at 650 °C for 2 h; (d) treated with RTA at 725 °C for 60 s. SEM images of PdO-functionalized ZnO:Pd samples at (e) lower and (f) higher magnification.

Figure 1(b-d) show SEM images at higher magnification of as-grown, TA (at 650 °C for 2 h), or RTA (at 725 °C for 60 s) treated films. The grain diameter in the case of as-grown samples is in the range of 200 – 300 nm, which is comparable with Fe-doped and Sn-doped ZnO nanostructured films reported previously¹¹⁻¹². After TA or RTA treatment the diameter of grains is slightly increased to 250 – 350 nm (see Figure 1(b-d)). The high roughness of grains can lead to higher surface-to-volume ratio which is very important for sensing applications¹⁷.

After functionalization using PdCl₂ aqueous solution and subsequent TA treatment the growth of nanoparticles (NPs) on the surface of ZnO:Pd grains was observed, see Figure 1e,f. The morphology of grains was not changed essentially. The diameter of NPs lies between 10 – 30 nm and the NPs density reaches a value of $\sim 0.4 \times 10^9 \text{ cm}^{-2}$. A previous work demonstrated by X-ray photoelectron spectroscopy (XPS) that these NPs are formed from PdO¹⁸. The surface content of PdO was determined to be $\sim 17\%$ ¹⁸.

Figure 2(a) show the room temperature Raman spectra of ZnO:Pd and PdO-functionalized ZnO:Pd nanostructured films. For both samples the two high intensity peaks at $\sim 99 \text{ cm}^{-1}$ and $\sim 437 \text{ cm}^{-1}$ were observed, which can be attributed to $E_2(\text{low})$ and $E_2(\text{high})$ modes of wurtzite structure of ZnO, respectively. The other peaks with lower intensity at ~ 203 , ~ 331 , ~ 382 , ~ 408 , ~ 574 , and $\sim 583 \text{ cm}^{-1}$ can be attributed to $E_2(\text{high})-E_2(\text{low})$, $A_1(\text{TO})$, $E_1(\text{TO})$, $E_2(\text{high})$ and $A_1(\text{LO})$ and $E_1(\text{LO})$ modes, respectively¹⁹. In the case of PdO-functionalized ZnO:Pd nanostructured films the additional peak at $\sim 650 \text{ cm}^{-1}$ was observed, which can be attributed to B_{1g} mode of PdO, which involves only oxygen lattice motion parallel to c -axis²⁰. The formation of PdO after TA treatment at 650 °C for 30 min can be explained by oxidation of Pd nanoparticles ($O_2 + 2Pd \rightleftharpoons PdO$)⁶. Also, it can be observed that the functionalization process does not induce essential changes in crystallinity of ZnO:Pd nanostructured films.

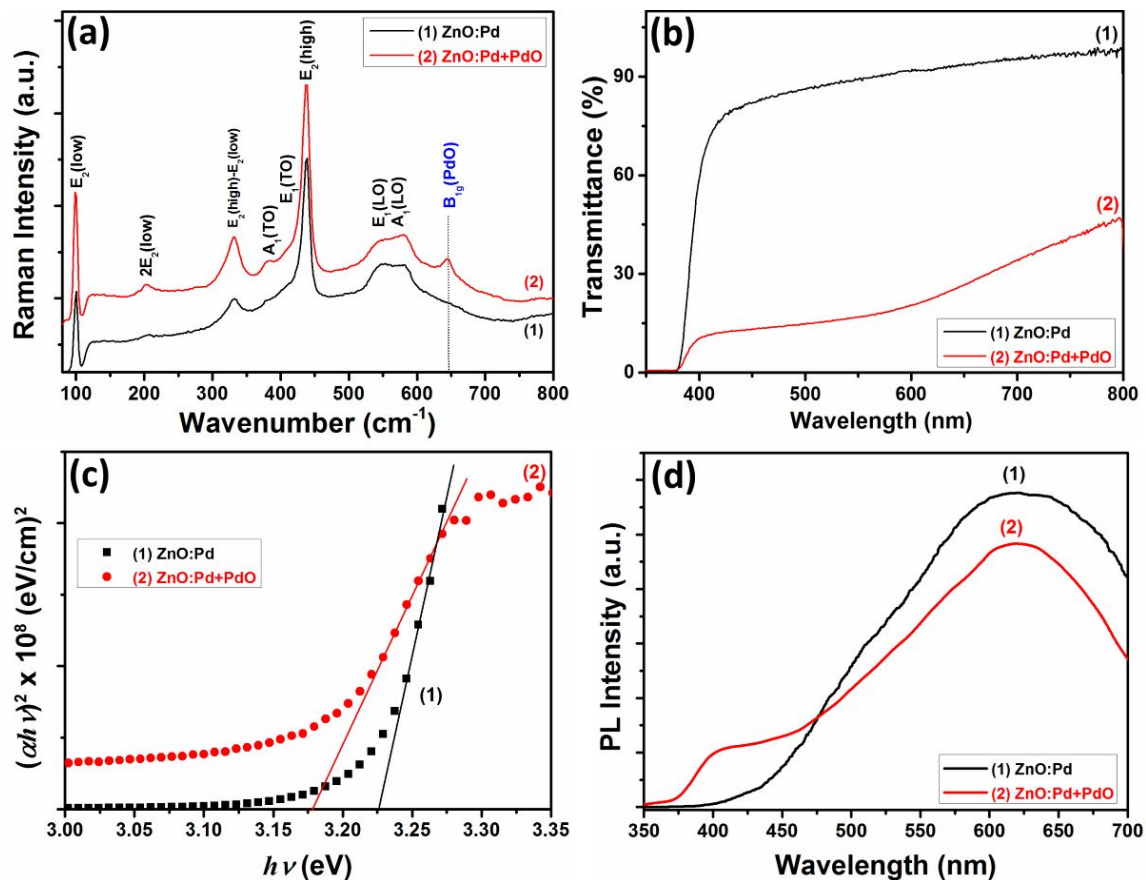


Figure 2. (a) Room temperature Raman spectra of ZnO:Pd and PdO-functionalized ZnO:Pd nanostructured films. (b) Transmission spectra of pristine ZnO:Pd and PdCl₂-functionalized nanostructured films and (c) respective plot of $(\alpha h\nu)^2$ vs. photon energy ($h\nu$). (d) Room temperature PL spectra of ZnO:Pd and PdO-functionalized ZnO:Pd nanostructured films

Figure 2(b) shows the optical transmittance spectra of ZnO:Pd and PdO-functionalized ZnO:Pd nanostructured films. In the case of ZnO:Pd sample the transmittance is higher than 80% in visible region. Previous study demonstrated that Pd content does not influence the transparency of ZnO:Pd nanostructured films in visible region¹⁸. By functionalization using PdCl₂ aqueous solution the considerable decrease of transparency in the visible region was observed (< 45%, see Figure 2(b)). This can be an indicator of improved visible light absorbance by adding PdO NPs, which was also observed for other metal oxides²¹. The values of the optical band gap (E_g) were obtained from the intercept of $(\alpha h\nu)^2$ vs. photon energy ($h\nu$) (see Figure 2(c)). From this *so called* tauc plot, for ZnO:Pd nanostructured films an E_g of ~ 3.22 eV was determined, while for functionalized sample the E_g value decreased slightly to ~ 3.17 eV. This can be a result of the overlapping of the corresponding ZnO and PdO components, as well as the reduced density of defects (annealing of intrinsic and extrinsic defects) and a slight increase in diameter of the crystallites after additional TA treatment at 650 °C for 30 min¹¹.

Figure 2(d) shows the room temperature PL spectra of ZnO:Pd and PdO-functionalized ZnO:Pd nanostructured films. In both cases the PL spectra is dominated by visible broad emission bands, and the near band edge emission (NBE) in the UV range is considerably reduced compared to the visible luminescence²². Emission bands in the visible regions for ZnO are quite complex and are related to defects and impurities, such as oxygen vacancies, Zn interstitials, oxide antisite defect, and zinc vacancies²³⁻²⁴. The study of defects in solids for photonic applications can be done by various techniques²⁵⁻²⁸. In the present case, yellow-orange emission bands at 620 nm is observed (see Figure 2(d))²⁹. Although defects at the origin of these bands are still controversial, the yellow emission (570 – 590 nm) is widely assigned to the doubly charged oxygen vacancy (V_{O}^{2+}) and the orange emission (590 – 620 nm) is commonly assigned to the interstitial oxygen (O_i) on the ZnO surface^{23, 29}. The O_i are mainly induced after annealing or the surface modifications²³.

The gas sensing properties of ZnO:Pd nanostructured films were investigated in detail in previous work and showed higher gas response to ethanol vapors in the operating temperature region of 200 – 400 °C, i.e. there is no selectivity to H₂ gas in this temperature region¹⁸. Therefore, they do not presents substantial interest for H₂ gas sensing applications and only PdO-functionalized ZnO:Pd nanostructured films will be investigated next. Figure 3(a) shows the gas response to different gases and vapors (1000 ppm of H₂ gas, 10 000 ppm of CH₄ gas, 1000 ppm of ethanol, acetone, *n*-butanol, 2-propanol, methanol and NH₃). Up to 200 °C operating temperature, the sample showed no response to other gases and vapors with exception of H₂ gas. The H₂ gas response at 25, 50, 100, 150 and 200 °C is ~ 2, ~ 6.7, ~ 6.4, ~ 12 and ~ 9.5, respectively. The dynamic response to 1000 ppm of H₂ gas at different operating temperatures is presented in Figure 3(b). The calculated response times at 25, 50, 100, 150 and 200 °C are ~ 175, ~ 80, ~ 70, ~ 50 and ~ 40 s, respectively, while the calculated recovery times at 25, 50, 100, 150 and 200 °C are > 800, ~ 400, ~ 300, ~ 120, and ~ 80 s, respectively. Thus, by increasing the operating temperature the response and recovery times of PdO-functionalized ZnO:Pd nanostructured films are decreasing. This can be explained based on increased thermal energy which become high enough to overcome the activation energy barrier of surface reactions³⁰.

The improved H₂ gas sensing properties of PdO-functionalized ZnO:Pd samples can be explained as followed. In the case of noble metal functionalized metal oxides, commonly, two concepts are involved. The electronic sensitization hypothesis assume the formation of additional depletion regions at the interface of *n*-type ZnO:Pd ($E_g = 3.3$ eV) and *p*-type PdO ($E_g = 1.1$ eV) due to different work functions of the materials¹⁷⁻¹⁸. This creates a higher modulation of conduction channel of ZnO:Pd grains under exposure to H₂ gas and therefore a higher response³¹. The second widely proposed mechanism of “chemical sensitization” can explain the improved H₂ gas sensing properties of PdO-functionalized ZnO:Pd nanostructured films much better. This mechanism assumes catalytic dissociation of molecular oxygen, which lead to a higher coverage of grains with atomic oxygen and to a greater and faster degree of electron withdrawal from the ZnO:Pd grains. This also explains very well the low operating temperatures due to high catalytic properties of PdO³¹.

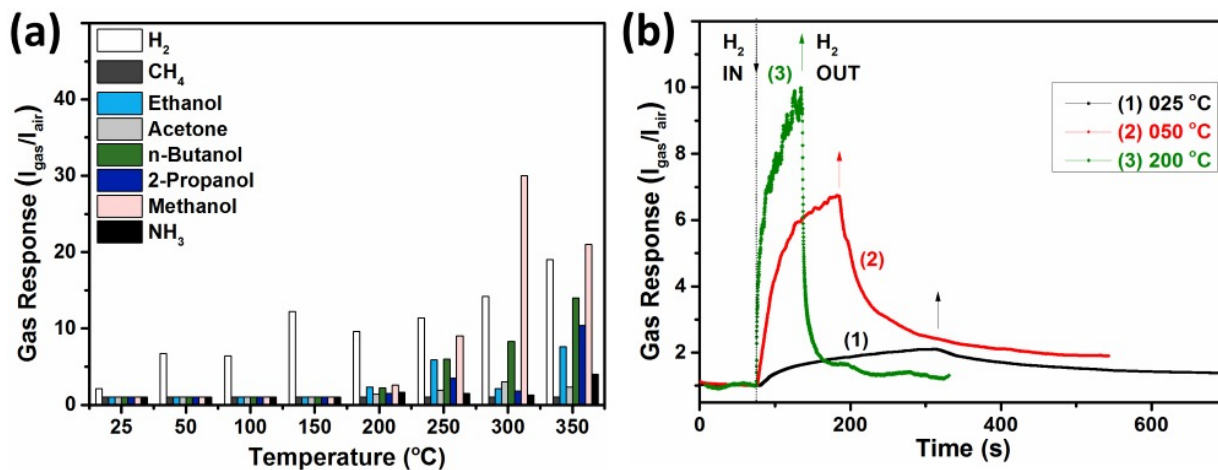


Figure 3. (a) Gas response versus operating temperature of PdO-functionalized ZnO:Pd nanostructured film. The concentration of gases and vapors is: H₂ – 1000 ppm, CH₄ – 10 000 ppm, ethanol, acetone, n-butanol, 2-propanol, methanol, NH₃ – 1000 ppm. (b) Dynamic gas response to 1000 ppm of H₂ at 25, 50, and 200 °C.

More detailed gas sensing mechanism of PdO-functionalized ZnO:Pd nanostructured films with representation of energy band diagrams and equations of different involved processes has been presented in a previous work¹⁸.

4. CONCLUSIONS

In summary, via a simple synthesis from chemical solutions (SCS) approach and post-growth TA and RTA treatment highly crystalline Pd-doped ZnO nanostructured films were synthesized. The morphological study demonstrated that the films are composed of interconnected columnar-type grains with rough surface and with a diameter in the range of 200 – 300 nm. PdO-functionalized samples were obtained using PdCl₂ aqueous solution and subsequent TA treatment at 650 °C for 30 min. We demonstrated that on the surface of ZnO:Pd grains the PdO NPs with diameter in range of 10 – 30 nm were grown. The presence of PdO phase was determined/evidenced by micro-Raman measurements. Gas sensing results showed that PdO-functionalization is a very efficient method to increase the selectivity of samples to H₂ gas. Up to 200 °C operating temperature the studied samples demonstrated no response to other reducing gases and vapors. Also, the response of ~ 2 was obtained even at room temperature, which is very important for low-power applications due to the exclusion of micro-heater.

Acknowledgements : Dr. Lupan gratefully acknowledges CNRS Council for support as expert scientist at IRCP Chimie ParisTech, Paris. This research was sponsored partially by the German Research Foundation (DFG) under the schemes PAK 902 (AD 183/12-1). This research was partly supported by the STCU within the Grant 6229.

REFERENCES

- Schlapbach, L.; Züttel, A., Hydrogen-Storage Materials for Mobile Applications. *Nature* **2001**, *414*, 353-358.
- Zhang, D.; Sun, Y. e.; Jiang, C.; Zhang, Y., Room Temperature Hydrogen Gas Sensor Based on Palladium Decorated Tin Oxide/Molybdenum Disulfide Ternary Hybrid Via Hydrothermal Route. *Sensors and Actuators B: Chemical* **2017**, *242*, 15-24.
- Xu, J.; Pan, Q.; Shun, Y. a.; Tian, Z., Grain Size Control and Gas Sensing Properties of ZnO Gas Sensor. *Sensors and Actuators B: Chemical* **2000**, *66*, 277-279.
- Bie, L.-J.; Yan, X.-N.; Yin, J.; Duan, Y.-Q.; Yuan, Z.-H., Nanopillar ZnO Gas Sensor for Hydrogen and Ethanol. *Sensors and Actuators B: Chemical* **2007**, *126*, 604-608.
- Yamazoe, N., New Approaches for Improving Semiconductor Gas Sensors. *Sensors and Actuators B: Chemical* **1991**, *5*, 7-19.
- Rashid, T.-R.; Phan, D.-T.; Chung, G.-S., A Flexible Hydrogen Sensor Based on Pd Nanoparticles Decorated ZnO Nanorods Grown on Polyimide Tape. *Sensors and Actuators B: Chemical* **2013**, *185*, 777-784.

7. Lupan, O.; Postica, V.; Labat, F.; Ciofini, I.; Pauporté, T.; Adelung, R., Ultra-Sensitive and Selective Hydrogen Nanosensor with Fast Response at Room Temperature Based on a Single Pd/Zno Nanowire. *Sensors and Actuators B: Chemical* **2017**, *254*, 1259-1270.
8. Drmosh, Q. A.; Yamani, Z. H.; Hossain, M. K., Hydrogen Gas Sensing Performance of Low Partial Oxygen-Mediated Nanostructured Zinc Oxide Thin Film. *Sensors and Actuators B: Chemical* **2017**, *248*, 868-877.
9. Zhong Lin, W., Zinc Oxide Nanostructures: Growth, Properties and Applications. *Journal of Physics: Condensed Matter* **2004**, *16*, R829.
10. Lupan, O.; Pauporte, T.; Viana, B.; Aschehoug, P.; Ahmadi, M.; Cuenya, B. R.; Rudzevich, Y.; Lin, Y.; Chow, L., Eu-Doped Zno Nanowire Arrays Grown by Electrodeposition. *Applied Surface Science* **2013**, *282*, 782-788.
11. Postica, V., et al., Morphology Dependent Uv Photoresponse of Sn-Doped Zno Microstructures. *Solid State Sciences* **2017**, *71*, 75-86.
12. Postica, V.; Hölken, I.; Schneider, V.; Kaidas, V.; Polonskyi, O.; Cretu, V.; Tiginyanu, I.; Faupel, F.; Adelung, R.; Lupan, O., Multifunctional Device Based on Zn:Fe Nanostructured Films with Enhanced Uv and Ultra-Fast Ethanol Vapour Sensing. *Materials Science in Semiconductor Processing* **2016**, *49*, 20-33.
13. Cretu, V.; Postica, V.; Mishra, A. K.; Hoppe, M.; Tiginyanu, I.; Mishra, Y. K.; Chow, L.; de Leeuw, N. H.; Adelung, R.; Lupan, O., Synthesis, Characterization and Dft Studies of Zinc-Doped Copper Oxide Nanocrystals for Gas Sensing Applications. *Journal of Materials Chemistry A* **2016**, *4*, 6527-6539.
14. Lupan, O.; Cretu, V.; Postica, V.; Polonskyi, O.; Ababii, N.; Schütt, F.; Kaidas, V.; Faupel, F.; Adelung, R., Non-Planar Nanoscale P-P Heterojunctions Formation in $Zn_xCu_{1-x}O_y$ Nanocrystals by Mixed Phases for Enhanced Sensors. *Sensors and Actuators B: Chemical* **2016**, *230*, 832-843.
15. Lupan, O., et al., Localized Synthesis of Iron Oxide Nanowires and Fabrication of High Performance Nanosensors Based on a Single Fe_2O_3 Nanowire. *Small* **2017**, *13*, 1602868.
16. Lupan, O., et al., Enhanced Ethanol Vapour Sensing Performances of Copper Oxide Nanocrystals with Mixed Phases. *Sensors and Actuators B: Chemical* **2016**, *224*, 434-448.
17. Postica, V., et al., Multifunctional Materials: A Case Study of the Effects of Metal Doping on Zno Tetrapods with Bismuth and Tin Oxides. *Advanced Functional Materials* **2017**, *27*, 1604676.
18. Postica, V.; Lupan, O.; Pauporté, T.; Adelung, R., Pd- and Pdo Modified Zno Nanostructured Films for Low Temperature Hydrogen Gas Sensing. *Sensors and Actuators B: Chemical* **2018**, *In progress*.
19. Cuscó, R.; Alarcón-Lladó, E.; Ibáñez, J.; Artús, L.; Jiménez, J.; Wang, B.; Callahan, M. J., Temperature Dependence of Raman Scattering in Zno. *Physical Review B* **2007**, *75*, 165202.
20. McBride, J. R.; Hass, K. C.; Weber, W. H., Resonance-Raman and Lattice-Dynamics Studies of Single-Crystal Pdo. *Physical Review B* **1991**, *44*, 5016-5028.
21. Li, Q.; Li, Y. W.; Wu, P.; Xie, R.; Shang, J. K., Palladium Oxide Nanoparticles on Nitrogen-Doped Titanium Oxide: Accelerated Photocatalytic Disinfection and Post-Illumination Catalytic "Memory". *Advanced Materials* **2008**, *20*, 3717-3723.
22. Lupan, O., et al., Hybridization of Zinc Oxide Tetrapods for Selective Gas Sensing Applications. *ACS Applied Materials & Interfaces* **2017**, *9*, 4084-4099.
23. Özgür, Ü.; Alivov, Y. I.; Liu, C.; Teke, A.; Reshchikov, M. A.; Doğan, S.; Avrutin, V.; Cho, S.-J.; Morkoç, H., A Comprehensive Review of Zno Materials and Devices. *Journal of Applied Physics* **2005**, *98*, 041301.
24. Roso, S.; Güell, F.; Martínez-Alanis, P. R.; Urakawa, A.; Llobet, E., Synthesis of Zno Nanowires and Impacts of Their Orientation and Defects on Their Gas Sensing Properties. *Sensors and Actuators B: Chemical* **2016**, *230*, 109-114.
25. Bessière, A.; Lecointre, A.; Benhamou, R. A.; Suard, E.; Wallez, G.; Viana, B., How to Induce Red Persistent Luminescence in Biocompatible Ca 3 (Po 4) 2. *Journal of Materials Chemistry C* **2013**, *1*, 1252-1259.
26. Lupan, O.; Pauporté, T.; Viana, B., Low-Temperature Growth of Zno Nanowire Arrays on P-Silicon (111) for Visible-Light-Emitting Diode Fabrication. *The Journal of Physical Chemistry C* **2010**, *114*, 14781-14785.
27. Rodríguez Burbano, D. C.; Sharma, S. K.; Dorenbos, P.; Viana, B.; Capobianco, J. A., Persistent and Photostimulated Red Emission in Cas: Eu²⁺, Dy³⁺ Nanophosphors. *Advanced Optical Materials* **2015**, *3*, 551-557.
28. Gourier, D.; Bessière, A.; Sharma, S. K.; Binet, L.; Viana, B.; Basavaraju, N.; Priolkar, K. R., Origin of the Visible Light Induced Persistent Luminescence of Cr³⁺-Doped Zinc Gallate. *Journal of Physics and Chemistry of Solids* **2014**, *75*, 826-837.
29. Xu, X.; Xu, C.; Lin, Y.; Li, J.; Hu, J., Comparison on Photoluminescence and Magnetism between Two Kinds of Undoped Zno Nanorods. *The Journal of Physical Chemistry C* **2013**, *117*, 24549-24553.
30. Chang, J. F.; Kuo, H. H.; Leu, I. C.; Hon, M. H., The Effects of Thickness and Operation Temperature on ZnO:Al Thin Film Co Gas Sensor. *Sensors and Actuators B: Chemical* **2002**, *84*, 258-264.
31. Kolmakov, A.; Klenov, D. O.; Lilach, Y.; Stemmer, S.; Moskovits, M., Enhanced Gas Sensing by Individual SnO₂ Nanowires and Nanobelts Functionalized with Pd Catalyst Particles. *Nano Letters* **2005**, *5*, 667-673.